

**\*\*FULL TITLE\*\***

ASP Conference Series, Vol. **\*\*VOLUME\*\***, © **\*\*YEAR OF PUBLICATION\*\***  
**\*\*NAMES OF EDITORS\*\***

## The Magellanic Stream to Halo Interface: Processes that shape our nearest gaseous Halo Stream

Lou Nigra,<sup>1,2</sup> Snežana Stanimirović,<sup>1</sup> J. S. Gallagher, III,<sup>1</sup>  
 Felix J. Lockman,<sup>3</sup> David L. Nidever,<sup>4</sup> Steven R. Majewski<sup>4</sup>

**Abstract.** Understanding the hydrodynamical processes and conditions at the interface between the Magellanic Stream (MS) and the Galactic halo is critical to understanding the MS and by extension, gaseous tails in other interacting galaxies. These processes operate on relatively small scales and not only help shape this clumpy stream, but also affect the neutral gas dynamics and transfer of mass from the stream to the halo, thus affecting metal enrichment and gas replenishment of the Galaxy. We describe an observational program to place constraints on these processes through high-resolution measurements of HI emission, HI absorption and H $\alpha$  emission with unprecedented sensitivity. Methods will include structural analysis, searching for cold gas cores in clumps and analyzing gas kinematics as it transitions to the halo. The latter method includes sophisticated spatial integration techniques to deeply probe the neutral gas, which we apply to a new HI map obtained from the Green Bank Telescope with the highest sensitivity HI observations of the MS to date. We demonstrate that the integration techniques enhance sensitivity even further, thus allowing detection of apparent MS gas components with density approaching that of the Galactic halo.

### 1 Introduction

The Magellanic Stream (MS) is our nearest major gaseous interaction remnant. It trails across much of the southern galactic sky for  $> 100^\circ$  behind the Magellanic Clouds (MCs), passing near the Southern Galactic Pole at its midpoint. The MS head is presumed to be nominally between 52 and 61 kpc away, the distances to the MCs established by Koerwer (2009) and Hilditch et al. (2005). The distance to the tip is not well-constrained but estimates are of the same order as distances to the MCs. These distances are about 15 times closer than the nearest extragalactic tidal features of the Andromeda system, therefore the MS presents us with the opportunity to closely study star formation potential (or lack thereof), mass transfer, and kinematics of a major interaction feature on fine scales inaccessible elsewhere. No signs of stars or even star formation have been found in the MS to date. The mean column density of the MS ranges

---

<sup>1</sup> Department of Astronomy, University of Wisconsin, Madison WI 53706, USA

<sup>2</sup> National Astronomy and Ionosphere Center, HC3 Box 53995, Arecibo, PR 00612 USA

<sup>3</sup> National Radio Astronomy Observatory, Green Bank, WV 24944-0002, USA

<sup>4</sup> Department of Astronomy, University of Virginia, Charlottesville, VA 22904-4325, USA

from  $4 \times 10^{18}$  to  $4 \times 10^{19} \text{ cm}^{-2}$  along its length, which is an order of magnitude below the tidal debris star-formation threshold ( $4 \times 10^{20} \text{ cm}^{-2}$ ) found by Maybhate et al. (2007). Unlike High Velocity Clouds (HVCs), whose  $\text{H}\alpha$  emission can be explained by Galactic UV radiation, the MS is brighter in  $\text{H}\alpha$ , particularly near the MCs, suggesting another ionizing source. Global models of the MS using Smoothed Particle Hydrodynamics (SPH) and N-Body techniques have reproduced its large-scale structure with some degree of success with the then-current assumption of multiple MC orbits of the Galaxy (Moore & Davis 1994; Connors et al. 2006; Mastropietro et al. 2005). The new measurement of MC proper motions by Kallivayalil et al. (2006a) and Kallivayalil et al. (2006b) led Besla et al. (2007) to propose the likelihood of unbound MC orbits. Subsequently, Mastropietro (2008) presented revised results for the new orbits.

Something that the global models do not capture is the very rich, fine-scale structure revealed in recent HI MS maps such as Putman et al. (2003) and Brüns et al. (2005). Even finer structure was revealed by Stanimirović et al. (2008) in a high-resolution map of the northern tip of the MS using the 305 m dish at Arecibo. These observations revealed extended fine filamentary structure and clumps down to the angular resolution of the telescope ( $3.5'$ ). They also highlighted the importance of Kelvin-Helmholtz and Thermal Instabilities in forming the clumpy structure of the MS. In addition, they revealed cooler cores in some clumps suggesting star formation potential and providing clues to halo pressure and dark matter confinement of these clumps. Processes are clearly at work on these small scales that could affect star formation, the transfer of gas to the halo, and also may provide additional drag affecting MS global dynamics.

The global simulations mentioned above can miss these processes since SPH can suppress instabilities due to smoothing (Agertz et al. 2007), and N-body simulations ignore gas processes altogether. Grid-based modeling can capture these small-scale instabilities better, exemplified by simulations exploring mechanisms for excess  $\text{H}\alpha$  emission in the MS (Bland-Hawthorn et al. 2007), galaxy replenishment (Bland-Hawthorn 2009; Heitsch & Putman 2009), and HVCs in the halo (Quilis & Moore 2001). Grid-based modeling on these scales is producing some exciting insights into the possible processes at work.

We present here a research program aimed at setting some observational constraints on these processes that act on the MS at its interface with the Galactic halo and then using them to test these models. Towards this end, we have obtained the most sensitive HI emission map of portions of the MS to date and have begun to analyze the structure and kinematics of the gas. We are in the process of obtaining high resolution, high sensitivity measurements of  $\text{H}\alpha$  emission for insight into higher energy processes at the halo interface, and HI absorption to look for cold gas cores and characterize gas temperatures.

## 2 Observations: Completed, ongoing and planned

We have completed a program at the Green Bank Telescope <sup>1</sup> (beamwidth = 9.1') where we obtained deep HI spectra across two separate 12 deg<sup>2</sup> regions. One region (Region 1) is located in the northern tip and the other (Region 2) is 20 deg further up in the mid-MS region. On-the-fly (OTF) mapping and in-band frequency switching was employed. Region 1 data have been reduced with a fairly successful initial pass at baseline removal resulting in a cube with 3.53' square pixels, and velocity resolution of 0.161 km sec<sup>-1</sup> from -200 to -518 km sec<sup>-1</sup>. Noise was measured at  $\sigma_T = 4.2$  mK corresponding to column density noise  $\sigma_N = 1.14 \times 10^{17}$  cm<sup>-2</sup> for a 15 km sec<sup>-1</sup> FWHM profile. At less than half the noise of the Galactic All-Sky Survey (GASS) (McClure-Griffiths et al. 2009) scaled to the same profile, the map presented here is the most sensitive of the MS to date. Column density and velocity field maps are shown in Figure 1.

Further plans include observations of the fine-scale signature of ionization process on selected clumps and features by obtaining deeply integrated, high-resolution H $\alpha$  observations. We will compare our results to those expected in models of ionization through Galactic UV radiation or energetic gas processes such as those proposed by Bland-Hawthorn et al. (2007). We also plan to obtain deep absorption measurements in the direction of several background radio sources within the tip of the MS coinciding with clumps identified by Stanimirović et al. (2008). In addition to possibly identifying cold, potentially star-forming cores, these sensitive absorption measurements through specific small-scale structures will provide useful constraints on the analysis of gas kinematics.

## 3 Results & Discussion

The Region 1 HI column density image of Figure 1 (left), shows the main filament extending from the lower left to the upper right, which is part of the longer filament S2 identified by Stanimirović et al. (2008). The Region 1 velocity field (Figure 1 right) shows the general velocity gradient of the main filament, but also reveals some differentiation in places, suggesting some complexity in the projected dimension. Several prominent and interesting features are labeled in Figure 1: (A) and (B) appear as head-tail clumps; (C) is a narrow filament that apparently connects to the main filament; (D) are a series of relatively dense “spokes” at the edge of the main filament; (E) is a large, apparently coherent cloud that is significantly more diffuse than other clumps of its size in the map. Most of these features (A through D) have a strong component transverse to the main filament, suggesting that this filamentary substructure may represent ram-pressure or ablation shreds coming off the main cloud. It is interesting to note that most of the transverse substructure appears in the form of short filaments, instead of diffuse cloud envelopes. In the future, these structures will be analyzed further both spatially and kinematically to see what the de-projected structures

---

<sup>1</sup> The Robert C. Byrd Green Bank Telescope is operated by the National Radio Astronomy Observatory, which is a facility of the US National Science Foundation operated under cooperative agreement by Associated Universities, Inc.

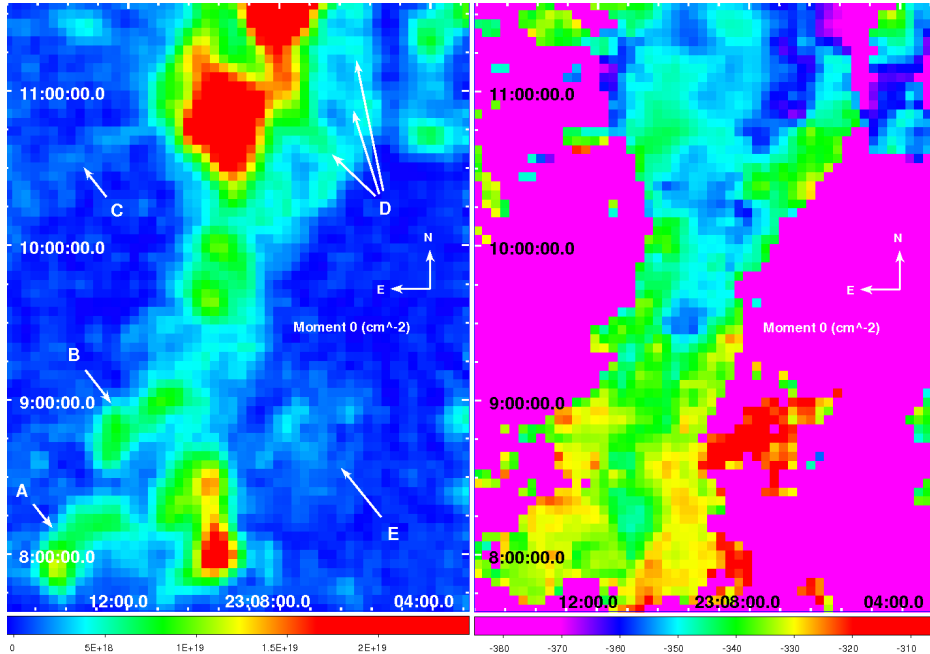


Figure 1. From Nigra et al. (2009, in prep.). Left - Region 1 column density map from the GBT data. Velocity range is  $-385$  to  $-305$   $\text{km sec}^{-1}$ . Intensity scale is  $0$  to  $2.5 \times 10^{19} \text{ cm}^{-2}$ . Features “A” through “E” are discussed in the text. Right - Region 1 velocity field for  $N_{HI} > 1.5 \times 10^{18} \text{ cm}^{-2}$ . See text for discussion. These images were generated with data from telescopes of the National Radio Astronomy Observatory, a National Science Foundation Facility, managed by Associated Universities, Inc.

might look like and what they might say about the processes at work here. We will also statistically compare the structure of this region to simulations from Bland-Hawthorn et al. (2007) by using Fourier Transform methods.

We are in the process of characterizing properties of the diffuse neutral gas in the MS-halo transition region. Profiles of gas properties (temperature and column density) as a function of distance from the clump centers will be compared with analytical and simulation results for various hydrodynamic processes, each of which will have a particular “signature” profile. For instance, the temperature vs. radial distance in an isolated cloud in the halo is quite different if experiencing saturated evaporation or if radiatively stabilized, as shown by Cowie & McKee (1977) and McKee & Cowie (1977).

These profiles are conventionally obtained by looking at observed spectra along a cross-section and fitting to a curve, as in Brüns et al. (2001). Further from the center, brightness decreases and velocity dispersion increases, causing measurement uncertainty to increase rapidly. In order to improve upon this method, we average spatially along a symmetry dimension under the assumption that the clump symmetry extends past its apparent boundaries. For instance, an isolated circular clump in a map is assumed spherical and can be integrated along concentric rings where each column of gas is nominally the same. Similarly

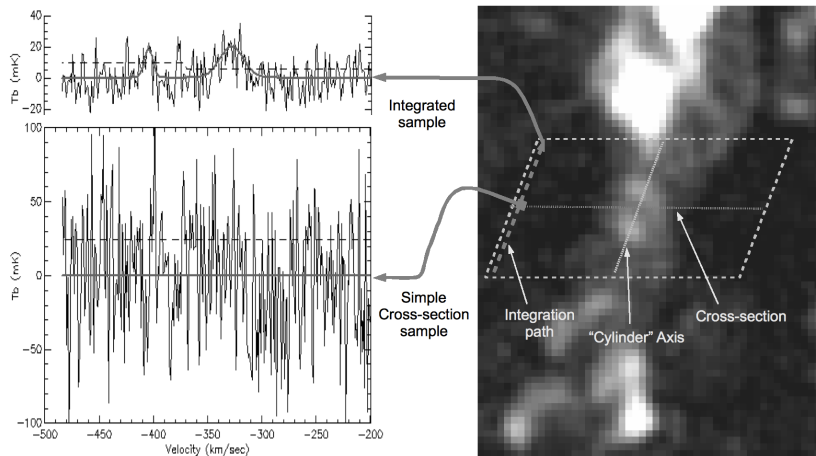


Figure 2. A demonstration of integration techniques used for gas analysis. A portion of the main filament is modeled as a cylinder. Integrating (averaging) parallel to its axis some distance away has two clearly detectable components while a single pixel spectrum at that distance has none.

for a linear feature, we assume cylindrical symmetry and average along lines parallel to the filament. More advanced techniques include integrating along  $N_{HI}$  contours or optimizing to fit a parametric 3D gas model.

To demonstrate the sensitivity of this approach, we show initial results from applying this method in Figure 2. Here a portion of the main filament of Region 1 is assumed to be roughly cylindrical along the axis indicated on the image. The spectra along a parallel path to the left were integrated (averaged) after removing the velocity gradient of the main filament. The spectrum sampled at a single location, as used in a simple cross-section profile, shows no sign of a detectable gas component, while the corresponding averaged spectrum of the cylindrical model clearly shows two gaussian components, with  $FWHM = 10$  and  $26 \text{ km sec}^{-1}$ , respectively. Each is detected well above their  $3\sigma$  detection limits (dashed line) with corresponding  $N_{HI} = 3.4 \times 10^{17} \text{ cm}^{-2}$  and  $1.1 \times 10^{18} \text{ cm}^{-2}$ , respectively.

Although detection of these apparent gas components clearly demonstrates the sensitivity of the technique, verification as actual low column density gas is still in progress. Their shape, width and velocity are roughly consistent with MS gas, and are not likely artifacts of the baseline procedure. However, at such high sensitivity, systematic artifacts not normally seen must be considered (Nidever et al. 2009, in prep.). Should either of these detections prove valid, it would suggest that a significant amount of low column density HI gas, well below thresholds of previous observations, exists in this part of the MS. If not, it will still establish unprecedented limits on a diffuse neutral gas component. In either case, this approach will provide valuable insight into the history, dynamics and hydrodynamic processes of the MS (Nigra et al. 2009, in prep.).

To gauge how close these detections are to the halo interface, an order of magnitude estimate of the number density is made. The filament's scale is  $\sim 1^\circ$  on the sky. Assuming a distance of  $\sim 60 \text{ kpc}$ , the scale width is then

$\sim 1$  kpc =  $3.1 \times 10^{21}$  cm. The number density for the 26 km sec<sup>-1</sup> FWHM component is then on the order of  $1.1 \times 10^{18} \div 3.1 \times 10^{21} = 3.5 \times 10^{-4}$  cm<sup>-3</sup>. This is on the same order as the upper range of ionized halo number density estimates (Sembach et al. 2003) and we can detect even weaker lines, so we may indeed be probing HI very close to the halo interface.

#### 4 Conclusions

The rich fine, clumpy and filamentary structure on arcminute scales revealed in modern HI maps of the MS are not reproduced in global SPH and N-body simulations. Observations and grid-based local simulations reveal that this structure is likely produced by hydrodynamical instabilities at the interface between the cool, stripped gas as it moves through the hot halo gas. These processes may be an important source of MS structure, a mechanism for ionizing the MS gas as well as a significant means of transferring gas from the MS to the halo, and eventually to the Galactic disk.

A program is in progress to place observational constraints on these processes and on the modeling of them by obtaining the most sensitive measurements to date of the MS gas in both HI and H $\alpha$  emission, as well as in HI absorption, on the periphery of the MS where it is closest to the ambient halo environment. We have already obtained maps of two regions of the MS with unprecedented sensitivity. Using these data, we have demonstrated spatial integration techniques allowing detection of HI components at densities of  $\sim 10^{-4}$  cm<sup>-3</sup>, within an order of magnitude of estimated halo density upper limits. We will apply these techniques to characterize gas kinematics and then compare to models to determine what processes are operating on the MS periphery.

**Acknowledgments.** The authors thank Carl Heiles for his invaluable participation in the absorption measurement program. LN thanks the National Astronomy and Ionosphere Center for pre-doctoral support. JSG thanks the University of Wisconsin Graduate School for partial support of this research.

#### References

- Agertz, O., et al. 2007, MNRAS, 380, 963  
 Besla, G., Kallivayalil, N., Hernquist, L., Robertson, B., Cox, T. J., van der Marel, R. P., & Alcock, C. 2007, ApJ, 668, 949  
 Bland-Hawthorn, J., Sutherland, R., Agertz, O., & Moore, B. 2007, ApJ, 670, L109  
 Bland-Hawthorn, J. 2009, IAU Symposium, 254, 241  
 Brüns, C., et al. 2005, A&A, 432, 45  
 Brüns, C., Kerp, J., & Pagels, A. 2001, A&A, 370, L26  
 Connors, T. W., Kawata, D., & Gibson, B. K. 2006, MNRAS, 371, 108  
 Cowie, L. L., & McKee, C. F. 1977, ApJ, 211, 135  
 Heitsch, F., & Putman, M. E. 2009, ApJ, 698, 1485  
 Hilditch, R. W., Howarth, I. D., & Harries, T. J. 2005, MNRAS, 357, 304  
 Kallivayalil, N., et al. 2006, ApJ, 638, 772  
 Kallivayalil, N., van der Marel, R. P., & Alcock, C. 2006, ApJ, 652, 1213  
 Koerwer, J. F. 2009, AJ, 138, 1  
 Mastrogiro, C., Moore, B., Mayer, L., Wadsley, J., & Stadel, J. 2005, MNRAS, 363, 509  
 Mastrogiro, C. 2008, arXiv:0810.4155

- Maybhate, A., et al. 2007, MNRAS, 381, 59  
McClure-Griffiths, N. M., et al. 2009, ApJS, 181, 398  
McKee, C. F., & Cowie, L. L. 1977, ApJ, 215, 213  
Moore, B., & Davis, M. 1994, MNRAS, 270, 209  
Nidever, D. et al. 2009, in preparation.  
Nigra, L., Stanimirović, S., Gallagher, J. S., III, et al. 2009, in preparation.  
Putman, M. E., Staveley-Smith, L., Freeman, K. C., Gibson, B. K., & Barnes, D. G.  
2003, ApJ, 586, 170  
Quilis, V., & Moore, B. 2001, ApJ, 555, L95  
Sembach, K. R., et al. 2003, ApJS, 146, 165  
Stanimirović, S., Hoffman, S., Heiles, C., Douglas, K. A., Putman, M., & Peek, J. E. G.  
2008, ApJ, 680, 276